Available online at www.sciencedirect.com
ScienceDirect
Journal of Nuclear Materials 367–370 (2007) 940–946
journal of nuclear materials
www.elsevier.com/locate/jnucmat

In situ SCC observation on neutron irradiated thermally-sensitized austenitic stainless steel

Junichi Nakano [a,*,1], Yukio Miwa [a], Takashi Tsukada [a], Shinya Endo [a], Koichiro Hide [b]

[a] Japan Atomic Energy Agency, Tokai-mura, Naka-gun, Ibaraki-ken 319-1195, Japan
[b] Central Research Institute of Electric Power Industry, Yokosuka-shi, Kanagawa-ken 240-0196, Japan

Abstract

To examine the crack initiation and growth of irradiation assisted stress corrosion cracking (IASCC), in situ observations of the specimen surface were conducted during slow strain rate testing (SSRT) in oxygenated high purity water at 561 K. Each specimen of type 304 stainless steel was treated by solution annealing (SA), thermal sensitization (TS) or cold working (CW). After neutron irradiation of 1.0×10^{26} n/m^2 ($E > 1$ MeV), the gage length section of specimen was observed through a window equipped in the autoclave of SSRT machine and images were recorded automatically at regular intervals. Crack initiation was observed immediately after the maximum stress during SSRT of each specimen. The ranking of mean crack growth rate based on the images was CW > TS > SA. The relative susceptibility to IASCC estimated by fraction of intergranular stress cracking on fracture surface was observe to be SA > TS > CW.

1. Introduction

Irradiation assisted stress corrosion cracking (IASCC) is one of the material issues for application of austenitic stainless steel (SS) to the international thermonuclear experimental reactor (ITER) [1]. From the view point of life management of structural materials of the first wall/shield blanket modules of ITER, it is important to examine the crack initiation and growth process of IASCC of SS. To evaluate a susceptibility to stress corrosion cracking (SCC) of SS, slow strain rate testing (SSRT) in a corrosive environment is often used, and in situ observations of the specimen surface during SSRT of unirradiated materials have been reported by other investigators [2–5]. By in situ observations during SSRT, it is possible to obtain visual information, e.g., the timing and location of crack initiation, number of introduced cracks, and the crack growth process. However, in situ observation of the surface of irradiated specimens in high temperature water has not previously been carried out because of many technical hurdles associated with remote handling in a hot cell. This paper reports in situ observations

* Corresponding author. Address: Tokai Research Establishment, Japan Atomic Energy Agency (JAEA), Tokai-mura, Naka-gun, Ibaraki-ken 319-1195, Japan or Institutt for Energiteknikk(IFE), Os Alle 13, N-1751, Halden, Norway. Tel.: +47 69 21 24 14; fax: +47 69 21 22 01.
E-mail address: junichin@hrp.no (J. Nakano).
[1] On loan to Halden Reactor Project from JAEA at present.

0022-3115/$ - see front matter © 2007 Elsevier B.V. All rights reserved.
doi:10.1016/j.jnucmat.2007.03.264

during SSRT for neutron irradiated type 304 SS in high temperature water and examines the behavior of IASCC initiation and growth on type 304 SS.

2. Experimental

2.1. Materials

Commercial-grade type 304 SS was used. The chemical composition was Fe–0.063C–0.50Si–0.98Mn–0.026P–0.015S–9.99Ni–18.65Cr–0.036N–<0.01Co in wt%. The material was treated by solution annealing (SA) at 1373 K for 60 min, thermal sensitization (TS) at 1023 K for 100 min followed by aging at 773 K for 24 h, or cold working (CW, 20%). Specimens for SSRT with 20 mm in gage length, 4 mm in width, and 1 mm in thickness were machined. The specimens were loaded in an irradiation capsule and irradiated at 323 K in the coolant water of the Japan Materials Testing Reactor (JMTR) for net 708 days. The fast neutron fluence was estimated at 1.0×10^{26} n/m^2 ($E > 1$ MeV).

2.2. SSRT and in situ observation

To study susceptibility to IASCC, SSRT of the irradiated specimens was conducted in oxygenated high purity water at 561 K in 9.0 MPa at a facility for post-irradiation examination at the Japan Atomic Energy Agency (JAEA). The applied strain rate was 1.7×10^{-7} s^{-1}. Dissolved oxygen (DO) concentration was controlled at 8 ppm. The flow rate of water was maintained at 3×10^{-2} m^3/h. In situ observation was performed during the SSRT through a window made of sapphire installed in the autoclave. The gage length section of specimen was observed automatically at regular intervals with a charge-coupled device (CCD) camera system with 2.1 mega-pixels. The resolution of the system was such that 0.016 mm can be distinguished by some digital treatments. The fracture surface of the specimens was examined using a scanning electron microscope (SEM) following the SSRT.

3. Results and discussion

3.1. Crack initiation and growth behavior

The results of SSRT are summarized in Table 1. The mean crack growth rate in Table 1 was defined using the following equation:

Table 1
Results of SSRT after neutron irradiation to 10^{26} n/m^2 ($E > 1$ MeV)

Specimen ID	Treatment	Yield stress (MPa)	Maximum stress (MPa)	Total elongation (%)	Fraction of IGSCC (%)	Fraction of TGSCC (%)	Reduction in area (%)	In situ observation	Number of introduced cracks	Stress at crack initiation (MPa)	Mean crack growth rate (mm/s)
F10	SA	522	528	3.7	100	–	12.4	Successful	2	518	4.8×10^{-5}
F12		586	591	3.8	100	–	16.4	Not successful	–	–	–
H12	TS	586	657	7.5	35.6	64.4	17.8	Successful	2	652	6.9×10^{-5}
G12	CW	772	832	4.6	16.6	71.1	25.6	Successful	1	818	8.4×10^{-5}

Mean crack growth rate (mm/s)

= gage width (4mm)

/(time from crack initiation to failure (s)). (1)

Stress–strain curves and images obtained during SSRT are shown in Fig. 1. Since the thickness of the oxide film on each specimen surface increased with increasing SSRT period, the amount of light reflected from the specimen decreased with time and digital treatments of the images were necessary to clarify the surface condition or crack morphology. Fig. 2 shows crack growth rates which were calculated from the change in crack length observed on the images obtained at 60 min intervals. On the irradiated SA material, the initiation of the 1st crack was observed at 518 MPa and the 2nd crack introduced on the other side just before the failure. The crack growth rate was in the range of 5.6×10^{-6}–1.2×10^{-4} mm/s. On the irradiated TS material, the initiations of the 1st and the 2nd cracks were observed at 652 and 637 MPa, respectively. Fig. 2(b) indicates some tendencies for one crack to advance while the other is relatively dormant. The process of crack growth was repeated alternately and the cracks finally combined to cause specimen failure. In the case of the irradiated CW material, the range of crack growth rate, 1.4×10^{-6}–2.4×10^{-4} mm/s, was greater and more irregular than that of the irradiated SA material. For the CW specimen, stress at crack initiation was the largest and time from crack initiation to failure was the smallest. Therefore, the ranking of mean crack growth rate was CW > TS > SA. Andresen [6,7] indicated that crack growth rate increased with yield strength for cold worked type 304 SS. The present results agree with Andresen's indication.

Tani et al. [4] reported that many cracks were observed during SSRT in high temperature water for unirradiated thermally-sensitized Type 304 SS and the first crack introduced when the stress reached 80–90% of the maximum stress. However, as common features of the specimens in this study, crack initiation was observed immediately after the maximum stress was reached. It is thought that the crack initiation for the irradiated materials would need a stress comparable to the maximum stress since whole hardness increased with irradiation hardening.

3.2. Susceptibility to IASCC based on fraction of intergranular stress corrosion cracking

Fig. 3 shows SEM photographs of the fracture surfaces and a schematic illustration of the fracture mode on each surface. The fracture surfaces of the irradiated SA and TS materials were wholly intergranular stress corrosion cracking (IGSCC) and a mixture of IGSCC and transgranular stress corrosion cracking (TGSCC), respectively. The fracture surface of the irradiated CW material showed changing of IGSCC–TGSCC-ductile fracture according to the extent of crack growth. A relationship between crack growth rate and fracture morphology is not apparent upon comparison of Figs. 2 and 3.

The fraction of SCC for each specimen treatment is shown in Fig. 4. The ranking of susceptibility to IASCC estimated by a fraction of IGSCC (%IGSCC) was observed to be SA > TS > CW. %IGSCC of the irradiated materials in this study is compared with data in the literature [8–10] as a function of neutron fluence in Fig. 5. Kodama et al. [11] reported that %IGSCC of the irradiated SA type 304 SS increased markedly at neutron fluences exceeding 10^{25} n/m^2 and reached about %IGSCC of 100% at around 10^{26} n/m^2. %IGSCC of the SA material in this study is consistent with their result at around a neutron fluence of 1×10^{26} n/m^2. It is the original %IGSCC of the irradiated SA material without any additional treatment.

Hide et al. [12] performed microchemical analyses on the irradiated TS material irradiated to 3×10^{25} n/m^2 and reported Cr depletion and enrichment of Ni, Si and P at grain boundaries. It was indicated that Cr depletion might be saturated at the fluence and %IGSCC at high fluence was only controlled by the element concentration at grain boundaries. Moreover, side surface observation of the irradiated specimens after SSRT and discussion regarding deformation characteristics of the SA, TS and CW materials were performed [8]. The SA material deformed homogeneously through the gage section while the CW material showed localized deformation with shearing to 45° direction from the loading axis. The deformation mode of the TS material changed from homogeneous to inhomogeneous deformation.

It is difficult for the CW material to deform homogeneously through the gage section because of high hardness. Coarse slips in the grains would

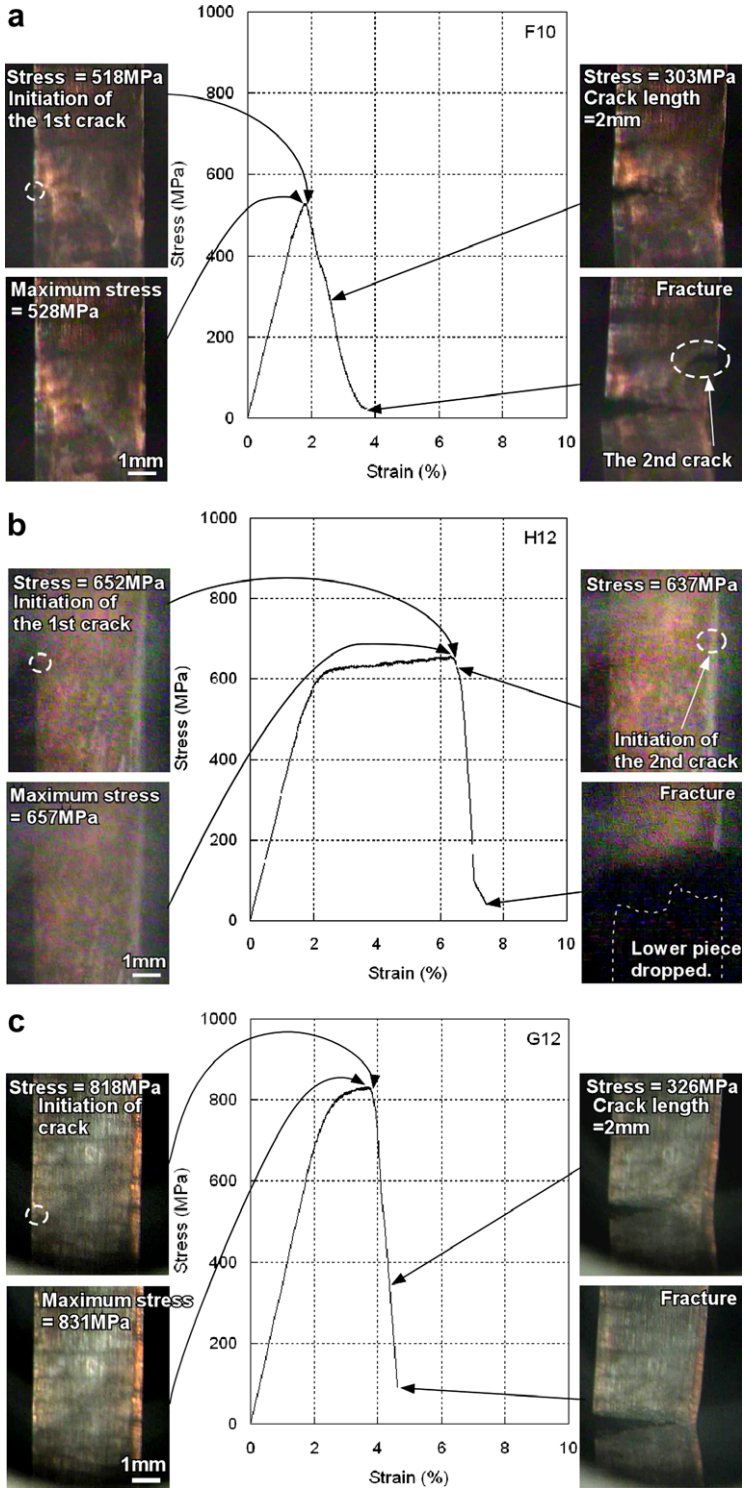

Fig. 1. Stress–strain curves and images obtained during the SSRT, (a) SA, (b) TS and (c) CW material.

be caused with shearing force and deformation would be localized. Consequently, true strain rate at the localized deformation region increases and TGSCC is introduced. On the other hand, the TS

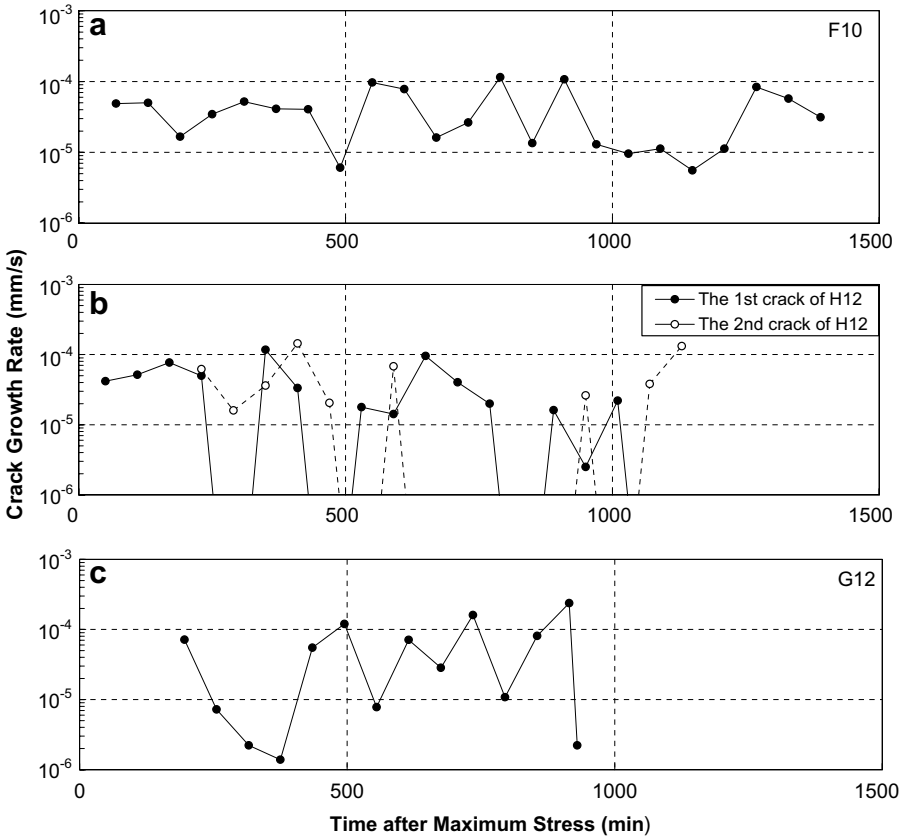

Fig. 2. Crack growth rate calculated from the images of in situ observation during the SSRT, (a) SA, (b) TS and (c) CW material.

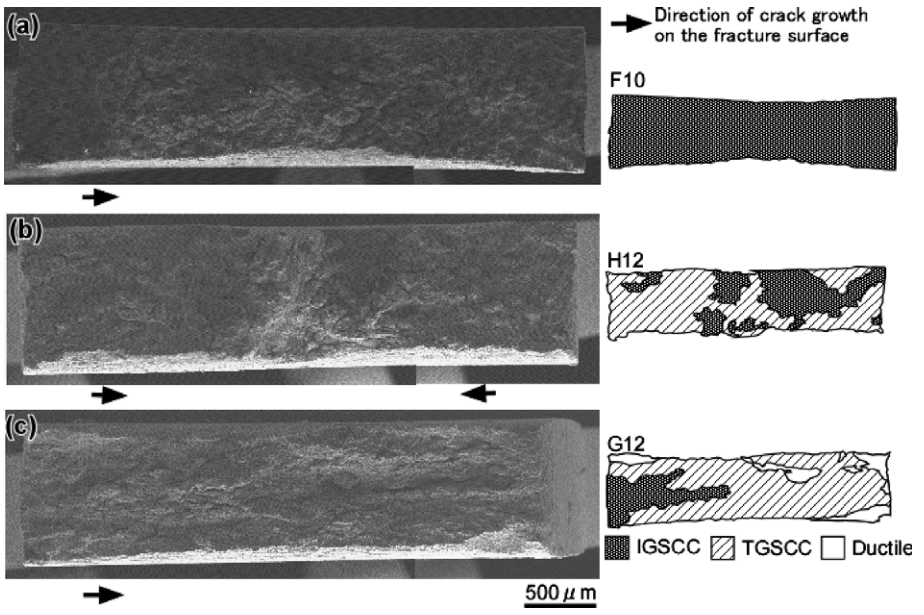

Fig. 3. Fracture surface and schematic illustration of the specimens, (a) SA, (b) TS and (c) CW material.

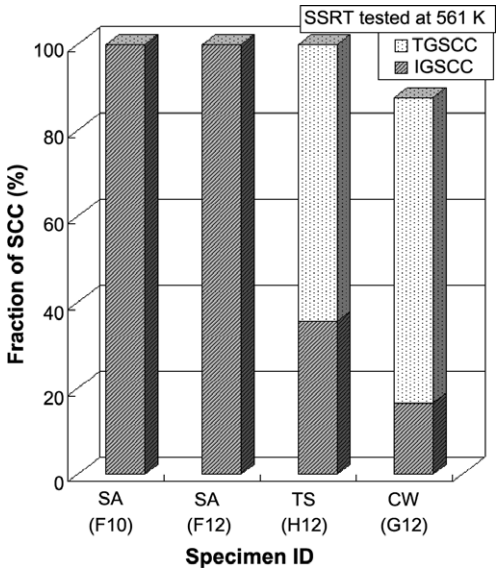

Fig. 4. Fraction of SCC after neutron irradiation to 10^{26} n/m^2 ($E > 1$ MeV).

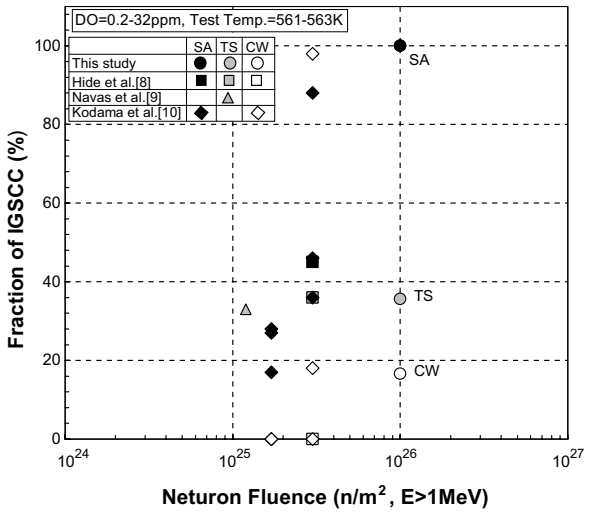

Fig. 5. Comparison of the fraction of IGSCC for irradiated type 304 SS [8–10].

material has chromium carbide precipitates at grain boundaries. Since the precipitates would slightly suppress homogeneous deformation, the TS material showed behavior between the SA and CW materials. The ranking of true strain rate indicated by Hide et al. [8] agrees with that of mean crack growth rate, i.e., CW > TS > SA. From the above, the susceptibility to IASCC based on %IGSCC would be relatively observed to be SA > TS > CW.

4. Conclusions

To investigate the behavior of crack initiation and growth, SSRT for type 304 SS irradiated to 1.0×10^{26} n/m^2 ($E > 1$ MeV) was conducted in oxygenated high purity water at 561 K. The material was treated by solution annealing, thermal sensitization or cold working. In situ observations during the SSRT and SEM examination of fracture surface after the SSRT were performed. From the results of these experiments, the following conclusions were drawn:

1. Crack initiation was observed immediately after reaching the maximum stress during SSRT of each specimen.
2. The ranking of mean crack growth rate based on the images was CW > TS > SA.
3. The relative susceptibility to IASCC based on %IGSCC was observed to be SA > TS > CW.

Acknowledgements

The authors would like to thank the JAEA staff of the Tokai WASTEF and Oarai hot laboratory, especially to T. Kohya, M. Numata, F. Takada and Y. Kato for their extensive post-irradiation examinations.

References

[1] ITER-EDA, Final Design Report, Materials Assessment Report, 1.1-1.3, 1999.
[2] T. Haruna, S. Zhang, T. Shibata, Corrosion (2004) 1104.
[3] T. Haruna, S. Zhang, T. Shibata, in: Proceedings of the 10th International Conference on Environmental Degradation of Materials in Nuclear Power Systems-Water Reactor, NACE, 2002 (CD-ROM).
[4] J. Tani, H. Hirano, S. Kato, Komae Research Laboratory Rep. No. T97014, Central Research Institute of Electric Power Industry, 1998 in Japanese.
[5] T. Fukumura, N. Nakajima, N. Totsuka, in: S. Ishino, B.L. Eyre, I. Kimura (Eds.), Proc. Mechanisms of Materials Degradation and Non-Destructive Evaluation in Light Water Reactors, INSS, Japan, 2002, p. 417.
[6] P.L. Andresen, Corrosion 2002, Paper No. 02509, NACE, 2002.
[7] P.L. Andresen, in: Proceedings of the 11th International Conference Environmental Degradation of Materials in Nuclear Systems, Stevenson, ANS, 2003 (CD-ROM). p. 870.
[8] K. Hide, M. Mayuzumi, T. Kusanagi, H. Tsuji, M. Narui, in: Proceedings of the 13th Asian–Pacific Corrosion Control Conference, Paper No.D-04, JSCE, 2003.
[9] M. Navas, M.L. Castano, D. Gomez-Briceno, T. Onchi, in: Proceedings of the 11th International Conference on Envi-

ronmental Degradation of Materials in Nuclear Systems, ANS, 2003 (CD-ROM), p. 1142.
[10] M. Kodama, J. Morisawa, S. Nishimura, K. Asano, S. Shima, K. Nakata, J. Nucl. Mater. 212–215 (1994) 1509.
[11] M. Kodama, R. Katsura, J. Morisawa, S. Nishimura, S. Suzuki, K. Asano, K. Fukuya, K. Nakata, in: R.E. Gold, E.P. Simonen (Eds.), Proceedings of the sixth International Symposium on Environmental Degradation of Materials in Nuclear Power Systems-Water Reactors, TMS, 1993, p. 583.
[12] K. Hide, T. Onchi, M. Mayuzumi, in: Proceedings of the 10th International Conference on Environmental Degradation of Materials in Nuclear Power Systems-Water Reactors, NACE, 2002, (CD-ROM).